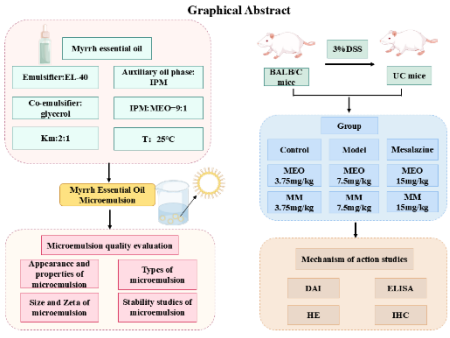
Journal of Oleo Science
Copyright ©2026 by Japan Oil Chemists' Society
doi : 10.5650/jos.ess25047
J. Oleo Sci. **75**, *(1) 51-66 (2026)*

Treatment of Ulcerative Colitis with Myrrh Essential Oil Microemulsion

Mengmeng Wang[1#], Tiantian Tang[2#], Mei Liu[1], Zihao Niu[1], Le Zhang[1], Xuan Wang[1], Ning Xia[1], Jie Wang[1], Jinhui Wang[1], Chao Chen[1], Xiaoxiao Ge[1], Qin Chen[1], Shihao Zhang[1], Huanxian Shi[1], Yundong Xie[1], Chongbo Zhao[1], Junbo Zou[1], Dongyan Guo[1], Yajun Shi[1], Ming Yang[3], Xiaofei Zhang[1]*, and Jing Sun[1]*

[1] *Key Laboratory of Basic and New Drug Research in Chinese Medicine, Shaanxi University of Chinese Medicine, 712046, Xianyang, Shaanxi, CHINA*
[2] *Department of Pharmacy, Xi'an Daxing Hospital, 710003 Xi 'an, Shaanxi, CHINA*
[3] *Key Laboratory of Modern Preparation of TCM, Ministry of Education, Jiangxi University of Traditional Chinese Medicine, 330004, Nanchang, Jiangxi, China is revised to 3 Key Laboratory of Modern Preparation of TCM, Ministry of Education, Jiangxi University of Traditional Chinese Medicine, 330004, Nanchang, Jiangxi, CHINA*

Abstract: Ulcerative colitis (UC) is a chronic inflammatory colon disease that is a major public health problem. The long-term administration of traditional drugs is likely to trigger adverse reactions. The myrrh essential oil (MEO) exhibits promising therapeutic efficacy against ulcerative colitis. However, due to the inherent instability and volatility of MEO, it was formulated into myrrh essential oil microemulsion (MM) with the aim of enhancing its stability. This study explored the optimal formulation for synthesizing MM, and a series of relevant indices were employed to meticulously investigate its stability characteristics. In animal experiments, a UC mouse model was established with the assistance of Dextran Sulfate Sodium (DSS). The therapeutic efficacy was comprehensively evaluated by recording Disease Activity Index (DAI) scores, detecting the levels of Tumor Necrosis Factor-α (TNF-α) and Interleukin-1β (IL-1β), and observing the morphological features of mouse colonic tissues through hematoxylin-eosin (HE) staining and immunohistochemistry (IHC) techniques. The results confirmed that both MEO and MM are effective in treating ulcerative colitis.



Keywords: myrrh essential oil, microemulsion, ulcerative colitis, stability

1 Introduction

UC is a chronic inflammatory colon disease. The lesions of UC predominantly localize within the large intestine, among which the rectum and sigmoid colon are the most frequently involved regions, and present a diffuse and continuous

Abbreviations: **UC**; ulcerative colitis, **MEO**; myrrh essential oil, **MM**; myrrh essential oil microemulsion, **HE**; Hematoxylin-eosin staining, **IHC**; immunohistochemistry, **TNF-α**; Tumor Necrosis Factor-α, **IL-1β**; Interleukin-1β, **DAI**; Disease activity index, **DSS**; Dextran Sulfate Sodium, **ELISA**; Enzyme-Linked Immunosorbent Assay, **GC-MS**; Gas Chromatography-Mass Spectrometry, **HLB**; Hydrophilic Lipophilic Balance, **IPM**; Isopropyl myristate, **IPP**; Isopropyl palmitate, **TEM**; transmission electron microscope, **RH-60**; Cremophor RH 60, **EL-40**; Cremophor EL 40, **PEG-400**; polyethylene glycol 400

# These authors have contributed equally to this work and share first authorship.
*Corresponding author: Xiaofei Zhang, Key Laboratory of Basic and New Drug Research in Chinese Medicine, Shaanxi University of Chinese Medicine, 712046, Xianyang, Shaanxi, CHINA. Jing Sun, Key Laboratory of Basic and New Drug Research in Chinese Medicine, Shaanxi University of Chinese Medicine, 712046, Xianyang, Shaanxi, CHINA.
E-mail: 2051028@sntcm.edu.cn (XZ), ph.175@163.com (JS).
Accepted October 24, 2025 (received for review February 23, 2025)
Journal of Oleo Science ISSN 1345-8957 print / ISSN 1347-3352 online
https://www.jstage.jst.go.jp/browse/jos/ https://mc.manuscriptcentral.com/jjocs

CC BY

distribution[1]. The principal clinical manifestations of UC include abdominal pain, constipation, bloody stools, weight loss, and severe ulceration[2]. Prolonged intestinal inflammation significantly increases the risk of colon cancer[3]. Its pathogenesis remains incompletely elucidated, but studies have shown that it is mainly associated with environmental factors, dietary elements, genetic determinants, intestinal flora imbalance, impairment of the intestinal mucosal barrier, and immune factors. In China, the prevalence rate of UC is approximately 11.6/100,000[4], and its incidence is on an upward trend[5]. Literature reports indicate that UC predominantly occurs in young adults. In summary, UC not only poses great challenges in treatment but also significantly reduces patients' quality of life.

Presently, the primary therapeutic medications for UC predominantly comprise immunosuppressants, biological agents, glucocorticoids, and amino acid salicylates. Nevertheless, their therapeutic efficacies is not satisfactory, and long-term use of these drugs will produce some adverse reaction[6]. In contrast, traditional Chinese herbal medicine, characterized by its multi-component, multi-target, and low toxicity, holds unique advantages in the treatment of this disease. Myrrh has numerous applications in fields such as medicine, pharmacy, and perfumery[7]. The main chemical constituents of myrrh encompass resin, gum and essential oil[8]. The pharmacological effects of MEO chiefly manifest as anti-inflammatory and anti-bacterial[9], and modern pharmacological studies have confirmed its antioxidant properties[10]. However, the physicochemical properties of essential oil are extremely unstable, it is prone to oxidation and volatilization. Consequently, essential oil is seldom formulated into a single preparation[11], which has substantially circumscribed its clinical application. Hence, the pursuit of stable-quality essential oil preparations has emerged as the focal point of research.

Currently, essential oils are mainly formulated into various dosage forms, such as gelling agent[12], inclusion compound[13], liposome[14], microemulsion[15], and submicron emulsion[16]. Microemulsion is a liquid dispersion system with a particle size ranging from 10-100 nm, composed of an oil phase, an emulsifiers and a co-emulsifiers mixed in specific proportions[17]. When essential oils are processed into microemulsions, their solubility can be improved, stability enhanced, and bioavailability increased[18]. Taking the (O/W) type microemulsion as an example: its outer phase is the water phase while the inner phase is the oil phase[19], the oil phase is encapsulated inside the colloid, so that the fat-soluble active components are protected from the influence of the external environment, such as oxygen, temperature, light, thereby improves its stability[20].

In conclusion, this study screened out the optimal prescription for the preparation of MM and conducted a comprehensive quality evaluation of it. Meanwhile, the anti-ulcerative colitis effects of MEO and MM were evaluated by DAI scores, the levels of inflammatory factors, HE staining of colonic tissues, and IHC detection of the expression of pivotal proteins within the inflammatory pathway.

2 Materials and Methods

2.1 Materials

Myrrh essential oil was purchased from Poli Aromatic Pharmaceutical Technology (Shanghai) Co., Ltd. Edible rapeseed oil was purchased from Sichuan Guanghan Oil & Fat Co., Ltd. Dextran sulfate sodium (0216011050) was purchased from MP Biomedicals. The p-JNK antibody (80024-1-RR) was purchased from Sanying Biotech (Wuhan) Co., Ltd. The p-ERK antibody (G1311004) was purchased from Seville (Shenzhen) Technology Co., Ltd. The DAB concentrate kit (DA1010) was purchased from Beijing Solarbio Science & Technology Co., Ltd. HRP-conjugated goat anti-rabbit antibody (111-035-003) was purchased from Jackson ImmunoResearch. TNF-α (MM-0132M1) and IL-1β (MM-0040M1) kits were purchased from Jiangsu Elisa Industry Co., Ltd. The particle size and zeta potential analyzer (Zetasizer Nano) was manufactured by Malvern (China) Instruments Co., Ltd. The transmission electron microscope (Hitachi HT7800) was manufactured by Hitachi Scientific Instruments (Beijing) Co., Ltd.

2.2 Animals

Specific pathogen-free (SPF) grade healthy male BALB/c mice (20 ± 2 g) were purchased from Chengdu Da Shuo Company Limited (Shaanxi Province, China) with an animal certificate number. SCXK (Chuan) 2020–030. Animal experiments were approved by the Animal Ethics Committee of Shaanxi University of Traditional Chinese Medicine, Xianyang, China (Number: SUCMDL20231031007).

2.3 GC-MS analysis of myrrh essential oil

Gas Chromatography-Mass Spectrometry (GC-MS) was employed to ascertain the chemical constituents of MEO. The operating conditions for GC-MS are detailed in the supporting materials.

2.4 Prescription selection of MM

2.4.1 Preparation of MM

Microemulsions were prepared by trans-phase emulsification method. Initially, the total prescription amount was tentatively set at 5 g, with the mixed oil phase and an auxiliary oil phase. The total emulsifier and the mixed oil phase were experimented in specific ratios (9:1-1:9). The effects of different emulsifiers, co-emulsifiers, oil phases, K_m values and temperature on microemulsions were investigated using single factor experiment. After uniformly mixing the oil phase and the emulsifier phase, water was gradually added under continuous stirring, while the electrical conductivity and temperature of the system were measured in real-time. During the experiment, with the increase of water addition, the electrical conductivity first rose to a peak; when the water addition exceeded a specific threshold, the electrical conductivity showed a trend of gradual decline. When the electrical conductivity reached the peak, the prepared microemulsion had the best stability, and the proportion of emulsifier, co-emulsifier and other components in the system at this time was the optimal formulation under such conditions. A pseudo-ternary phase diagram was plotted based on the dosage of this optimal formulation, and the best microemulsion preparation process and the proportion of each component could be further determined by quantitative analysis of the area of the microemulsion region in the phase diagram.

2.4.2 Selection of emulsifiers

Emulsifiers, which belongs to the category of surfactants, exhibits both hydrophilic and lipophilic properties and possesses the ability to blend immiscible liquids. Isopropyl myristate (IPM) was first used as the auxiliary oil phase and combined with MEO in a ratio of 9:1 to form the mixed oil phase. Cremophor EL 40 (EL-40), Cremophor RH 60 (RH-60), Tween-80 and Tween-20 were selected as candidate emulsifiers for the experiments, the rationale behind this selection lay in the fact that their HLB values were all between the range of 8-18, and it is generally acknowledged that the higher the HLB value, the stronger the hydrophilicity of the emulsifier. The conductivity experiment was performed following the method outlined in Section 2.4.1. By integrating this with a comparative analysis of the microemulsion region areas in the pseudo-ternary phase diagrams, the optimal emulsifier type was ultimately identified.

2.4.3 Selection of co-emulsifiers

Co-emulsifiers improve the stability of microemulsions by adjusting the HLB value of the emulsifier and changing the polarity of the system. In order to investigate the effect of co-emulsifiers on the formation of microemulsions, polyethylene glycol 400 (PEG-400), glycerol, ethanol and 1,2-propanediol were selected as candidate co-emulsifiers. Conductivity measurements were carried out according to the protocol detailed in Section 2.4.1. This experimental data, when combined with a comparative assessment of the microemulsion domain areas within the pseudo-ternary phase diagrams, enabled the final identification of the most suitable co-emulsifier type.

2.4.4 Selection of the oil phase

The types of auxiliary oil phases, namely oleic acid, isopropyl palmitate (IPP) and IPM, were employed in this study. Each of them was combined with MEO in a 9:1 ratio to formulate the corresponding mixed oil phases. The conductivity experiment was conducted using the method described in Section 2.4.1. Combined with a comparative analysis of the microemulsion region areas in the pseudo-ternary phase diagrams, the optimal oil phase was finally determined.

2.4.5 Selection of K_m values

The K_m value represents the ratio of emulsifier and co-emulsifier. It has been observed that during the microemulsion preparation process, variations in K_m values can result in substantial disparities in the characteristics of microemulsions. Consequently, a series of K_m values, namely 4:1, 3:1, 2:1, and 1:1. The optimal K_m value was determined by conducting the experiment described in Section 2.4.1.

2.4.6 Selection of temperature

Temperature is an important influencing factor for essential oil. Therefore, it is imperative to explore the preparation of microemulsions under diverse temperature conditions. To this end, the temperature parameters were designated as 25 °C, 30 °C, 40 °C, and 50 °C. The optimal temperature was determined by conducting the experiment described in Section 2.4.1.

2.5 Quality evaluation of MM

2.5.1 Appearance of microemulsion

Using tweezers, take out the copper mesh with a carbon-plated support film, and place approximately 10 μL of MM on the carbon film. After 10 minutes, blot away the excess microemulsion with filter paper. Then add the prepared phosphotungstic acid reagent, let it stand for 90 seconds, wipe off the excess reagent, and observe with a transmission electron microscope (TEM) after drying.

2.5.2 Type of microemulsion

Add appropriate amounts of Sudan III and methylene blue separately to the MM, and observe their diffusion rates: in

an O/W microemulsion, methylene blue diffuses faster than Sudan III; in a W/O microemulsion, methylene blue diffuses slower than Sudan III.

2.5.3 Determination of particle size and Zeta potential of microemulsion

Three batches of MM were prepared. For each batch, 1 mL of the sample was diluted 10-fold, followed by taking 1.3 mL of the diluted sample to measure the particle size using a particle size and zeta potential analyzer.

Three batches of MM were prepared, 1 mL of each was diluted 10 times, and 1.3 mL was taken to measure the potential with a particle size and zeta potential analyzer.

2.5.4 Physical stability of microemulsion

Three batches of MM were prepared. From each batch, 5 mL MM were transferred into centrifuge tubes and placed in a high-speed centrifuge. The centrifuge was set to 10,000 rpm and run for 15 minutes. After centrifugation, the microemulsion's appearance was closely examined to verify its retention of clarity and transparency, and to check for any oil-water separation.

2.5.5 Thermodynamic stability of microemulsion

2.5.5.1 Heating-cooling cycle experiment

Three batches of MM were prepared. For each batch, 5 mL of the microemulsion was taken in a centrifuge tube. The samples were first incubated at 40 °C for 24 h and then transferred to a 4 °C for another 24 h. The procedure was repeated six times. Subsequently, to observe the properties of the microemulsion.

2.5.5.2 Freeze-thaw cycle experiment

Three batches of MM were prepared, 5 mL of each batch was taken in a centrifuge tube and placed at -20 ℃ for 24 h, and then at room temperature for 24 h. The procedure was repeated six times to observe the properties of the microemulsion.

2.5.6 Accelerated stability experiment

Three batches of MM were prepared. For each batch, 5 mL was placed in a weighing bottle, sealed and placed in an environment with the temperature of 28 ℃-32 ℃, and humidity of 60%-70% for 3 months. During the entire storage period, samples were taken out at the end of each month for comprehensive testing to monitor changes in appearance, conductivity, and particle size.

2.5.7 Determination of essential oil retention in MEO and MM under thermal conditions

MM 320.00 g (MEO:1 g: EL-40:60 g, glycerine:30 g, IPM:9 g, water:220 g). Blank microemulsion 320.00 g (EL-40:60 g, glycerine:30 g, IPM:9 g, water:221 g). Aqueous-MEO 320.00 g (MEO:1 g, water:319 g)

According to the aforementioned method, three groups were prepared for each of the three samples, with each group placed in a 500 mL evaporating dish and then put into an oven at 60 °C. The three groups of samples were kept for 1 h, 3 h, and 8 h respectively. After reaching the corresponding drying time, they were taken out and weighed. Distilled water was added to make the total mass 1000 g, and the mixture was transferred to a 2000 mL round-bottomed flask. Volatile components were extracted using the steam distillation method until their volume no longer increased. The volatile components of each group were collected and their masses were recorded. The experiment was performed in triplicate, and the retention rate was calculated.

Volume of essential oil of MM = Volume of volatile components of MM - Volume of volatile components of Blank microemulsion. (1-1)

Essential oil retention = Essential oil volume of each sample at each time point/1.00 g*100%. (1-2)

2.6 Evaluation of the efficacy of myrrh essential oil microemulsion

2.6.1 Establishment of DSS-induced UC model in mice

90 SPF-grade healthy male BALB/c mice (20 ± 2 g), were randomly divided into nine groups, namely the Control group, Model group, Mesalazine group, MEO low-dose group, MEO medium-dose group, MEO high-dose group, MM low-dose group, MM medium-dose group, and MM high-dose group. In the MEO group, different doses of myrrh essential oil were diluted with rapeseed oil. In the MEO group, different doses of myrrh essential oil were diluted with rapeseed oil. The MM group was prepared by mixing myrrh essential oil with emulsifier (EL-40), co-emulsifier (glycerol), and mixed oil phase (IPP) under the conditions of K_m=2:1 and 25℃, and synthesizing microemulsions with different drug-containing doses according to the method in section 2.4.1. Mice in the Control group drank water and other groups drank 3% DSS solution for modelling. Administered after the second day of modelling. The Control group was administered rapeseed oil by gavage. The Mesalazine group was administered Mesalazine by gavage at a concentration of 600 mg/kg. MEO low dose and MM low dose groups (3.75 mg/kg), MEO medium dose and MM medium dose (7.5 mg/kg), and MEO high dose group and MM high dose (15 mg/kg) were administered for 7 days. During this time, the DAI was scored daily. At the

end of the final administration, all mice were fasted for 24 h. Subsequently, they were anesthetized with isoflurane, and blood was collected from their eyeballs. The collected blood was then centrifuged at 4 °C and 4000 r/min for 10 minutes to obtain serum, which was aliquoted and stored at -20 °C. After that, the mice were euthanized, and the colon was dissected. The natural length of the colon was measured and recorded[21]. One part of the colon was fixed with paraformaldehyde, and the other part was quick-frozen with liquid nitrogen and transferred to -80 °C[22, 23].

2.6.2 HE staining of mice colonic tissue

The colonic tissues of mice in each group were taken, subjected to gradient ethanol dehydration and paraffin embedding, followed by sectioning. The sections were first stained with hematoxylin, then counterstained with eosin, subsequently dehydrated until transparent and mounted, and finally observed for their morphology under a microscope.

2.6.3 TNF-α and IL-1β ELISA Assays

The ELISA was used to determine the levels of TNF-α and IL-1ß within mice serum. Firstly, the frozen serum was removed and TNF-α and IL-1ß were detected according to the kit instructions. Finally, the levels of each index were measured at 450 nm.

2.6.4 Immunohistochemical detection of p-JNK and p-ERK protein expression in the colon of mice

Mouse colon tissues from each group were fixed in 4% paraformaldehyde, followed by routine washing, dehydration, paraffin infiltration, embedding, and sectioning. The sections were deparaffinized in xylene and then hydrated through a graded ethanol series. Subsequently, the sections were immersed in 0.01 M citrate buffer, heated to boiling in a microwave, maintained at a gentle boil for 10 minutes, slowly cooled to room temperature, and washed 3 times with PBS. 3% hydrogen peroxide was added dropwise, incubated at room temperature for 15 minutes, and then washed 3 times with PBS. After blotting off the surrounding moisture with filter paper, non-immune normal goat serum was added dropwise to block non-specific antigens, and then primary antibodies (p-JNK or p-ERK) were added. The sections were incubated overnight at 4 °C in a humidified chamber. The next day, the sections were left at room temperature for 40 minutes and washed with PBS. Horseradish Peroxidase (HRP)-conjugated secondary antibody (rabbit anti-) was added, incubated at 37 °C for 1 hour, and then washed 3 times with PBS. After DAB staining, the sections were counterstained with hematoxylin, dehydrated through a graded ethanol series, cleared twice in xylene, air-dried, mounted with neutral gum, and finally examined under a microscope.

2.7 Statistical analysis

All experimental data in this study were submitted to statistical analysis using GraphPad Prism 9.0 software, and one-way analysis of variance (ANOVA) was used to compare differences between groups. $P < 0.05$ was considered statistically different.

3 Results

3.1 Identification of the composition of myrrh essential oil

The components of the MEO were identified by GC-MS, and its total ion flow diagram is shown in **Fig. 1**. The specific composition is mentioned in **Table 1**. The main compounds are shown in **Fig. 2**. Sesquiterpenes are the main components of myrrh essential oil[24]. Among the isolated and identified compounds, there are 14 sesquiterpenes, accounting for 81.08% of the total area. The main sesquiterpene components include Furanoeudesma-1,3-diene (24.19%), Curzerene (20.25%), Lindestrene (9.30%), Isolongifolene (7.15%), and ß-Elemene (7.38%)[25].

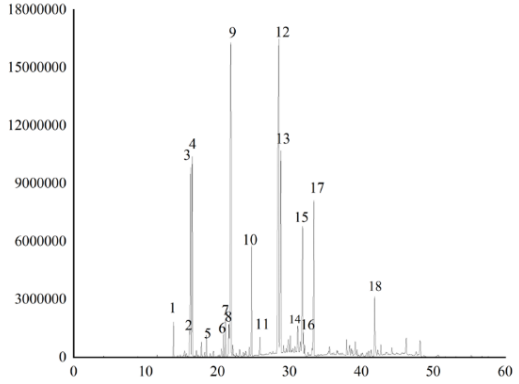


Fig. 1 Total Ion Flow Chart (TIC) of myrrh essential oil.

Table 1 The composition of myrrh essential oil.

No.	Compound	CAS	RI	Pct Total	Qual
1	δ-elemene	20307-84-0	1337	1.1363	97
2	β-Bourbonene	5208-59-3	1385	0.8393	91
3	Isolongifolene	1135-66-6	1388	7.1470	99
4	β-Elemen	515-13-9	1393	7.3848	91
5	γ-Elemene	29873-99-2	1432	0.7790	98
6	Germacrene D	23986-74-5	1478	0.8641	98
7	β-Eudesmene	17066-67-0	1483	1.5473	99
8	γ-Selinene	515-17-3	1493	1.1610	95
9	Curzerene	17910-09-7	1498	20.2477	96
10	Germacrene B	15423-57-1	1552	4.3622	99
11	Menthofuran	494-90-6	1574	0.7392	72
12	Furanoeudesma-1,3-diene	87605-93-4	1624	24.1935	99
13	Lindestrene	2221-88-7	1630	9.3001	99
14	Aromadendrene	489-39-4	1674	1.4322	87
15	Atractylone	6989-21-5	1687	7.9616	86
16	Germacrone	6902-91-6	1690	0.6908	95
17	(*R*,5*E*,9*E*)-8-Methoxy-3,6,10-trimethyl-4,7,8,11-tetrahydrocyclodeca[b]furan	108376-98-3	1717	7.2589	99
18	4-Benzyloxyaniline	6373-46-2	1810	2.9548	18

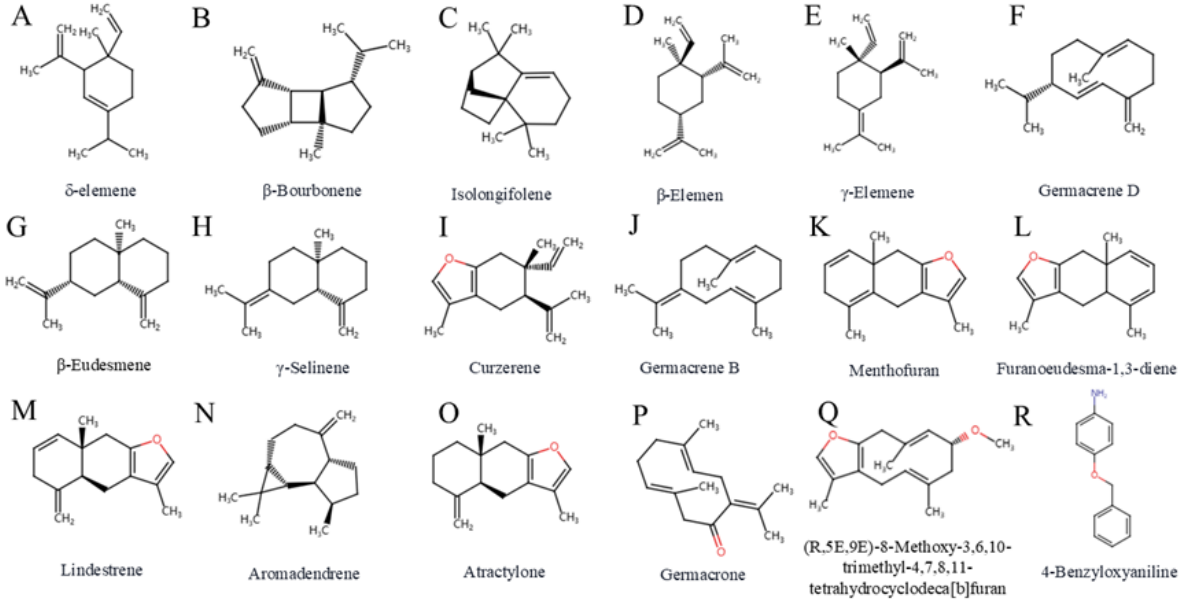


Fig. 2 (A-R) Shows the structure of specific compounds contained in myrrh essential oil.

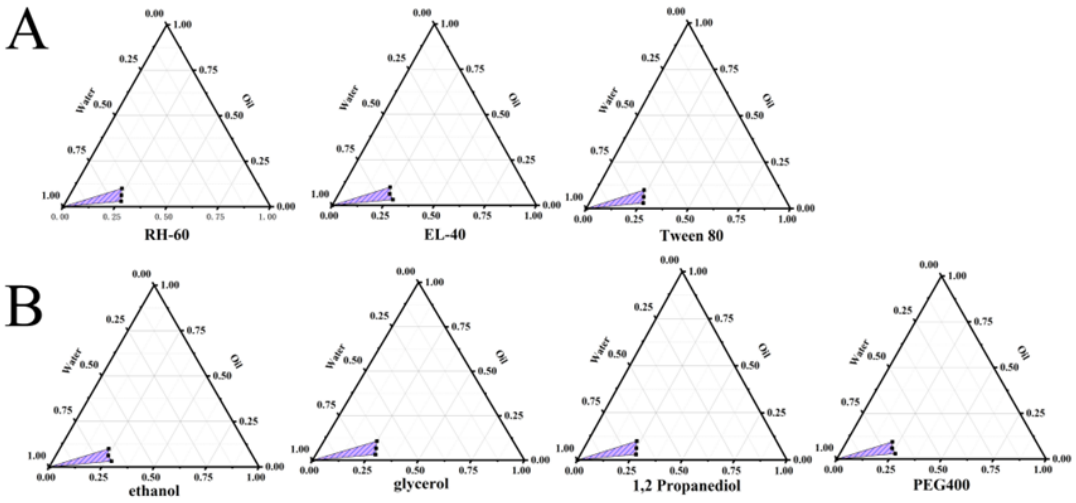


Fig. 3 Pseudo-ternary phase diagram of emulsifiers and co-emulsifiers. A: Pseudo-ternary phase diagram of emulsifiers, B: Pseudo-ternary phase diagram of co-emulsifiers.

3.2 Selection results of MM preparation

3.2.1 Selection of optimal emulsifiers

The preparation temperature was tentatively set at 25 °C. The auxiliary oil phase selected was IPM, which was mixed with MEO at a ratio of 9:1. EL-40, RH-60, Tween-80 and Tween-20 were used as candidate emulsifiers and the results are shown in **Fig. 3A**. The microemulsion area was $S_{EL\text{-}40} = 0.010091 > S_{Tween\text{-}80} = 0.009804 = S_{RH\text{-}60} = 0.009804$, respectively, and Tween-20 could not form a microemulsion as an emulsifier, so it was excluded. The experiment showed that the emulsifier EL-40 had the largest microemulsion area, clear and homogeneous appearance, which was determined to be the optimal emulsifier.

3.2.2 Selection of optimal co-emulsifiers

EL-40 was selected as the emulsifier, with the preparation temperature set at 25°C. The ratio of IPM to MEO was 9:1, and the K_m value was 2:1. The candidate co-emulsifiers included PEG-400, glycerol, ethanol and 1,2-propanediol. The results are shown in **Fig. 3B**. The microemulsion area was as follows: $S_{glycerol} = 0.011161 > S_{ethanol} = 0.010091 > S_{1,2\text{-}propanediol} = 0.009804 > S_{PEG\text{-}400} = 0.008921$. The experiments showed that when glycerol was used as a co-emulsifier, the area of microemulsion formation was the largest, and the microemulsion was clear and homogeneous in appearance, which was determined to be the optimal co-emulsifier.

3.2.3 Selection of optimal auxiliary oil phase

The emulsifier was EL-40, the co-emulsifier was glycerol, the preparation temperature was tentatively set at 25 °C with a K_m value of 2:1. Oleic acid, IPP, and IPM were used as candidate auxiliary oil phases, and the results are shown in **Fig. 4A**. The microemulsion area was $S_{IPM} = 0.011161 > S_{IPP} = 0.010463 > S_{oleic\ acid} = 0.004467$. The experiments showed that when IPM was used as the co-emulsifier, the microemulsion area was the largest, and the appearance was clear and homogeneous, which was determined to be the optimal auxiliary oil phase.

3.2.4 Selection of optimal K_m values

The emulsifier was EL-40, the co-emulsifier was glycerol, the auxiliary oil phase was IPM, and the preparation temperature was 25 °C. The K_m was examined for 4:1, 3:1, 2:1 and 1:1, and the results are shown in **Fig. 4B**. The microemulsion area was as follows: $S_{2:1} = 0.011161 > S_{1:1} = 0.010764 > S_{3:1} = 0.010463 = S_{4:1} = 0.010463$, and the experiments showed that the microemulsion area was the largest and the appearance of the microemulsion was clear and homogeneous when the K_m=2:1, which was determined to be the optimal K_m.

3.2.5 Selection of optimal preparation temperature

The emulsifier was EL-40, the co-emulsifier was glycerol, the auxiliary oil phase was IPM, and the K_m was 2:1. The preparation temperatures of 25 °C, 30 °C, 40 °C, and 50 °C were examined. The results were shown in **Fig. 4C**. The microemulsion areas were as follows: $S_{25\,°C} = 0.011161 > S_{30\,°C} = 0.09804 > S_{50\,°C} = 0.009227 > S_{40\,°C} = 0.007767$. The experiments showed that the microemulsion area was the largest at 25 °C, and the appearance was clarified and homogeneous, which was determined as the optimal temperature.

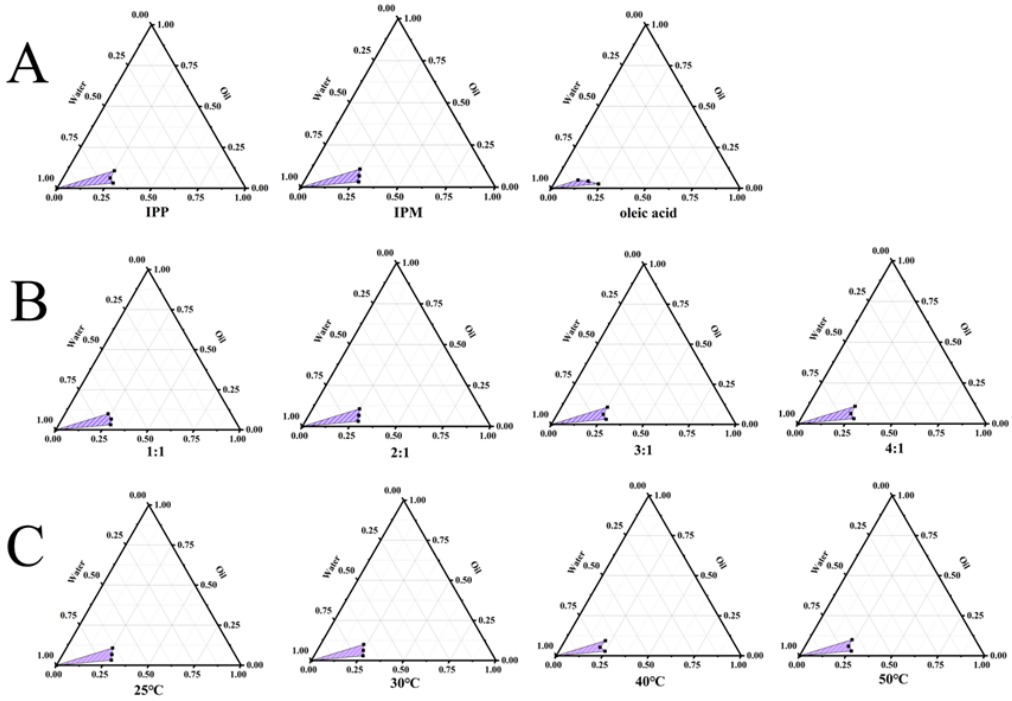


Fig. 4 Pseudo-ternary phase diagram of auxiliary oil phases, Km values and temperature. A: Pseudo-ternary phase diagram of auxiliary oil phases, B: Pseudo-ternary phase diagram of Km values, C: Pseudo-ternary phase diagram of temperature.

3.3 Quality evaluation of myrrh essential oil microemulsion preparation system

3.3.1 Appearance of microemulsion

The appearance of MM was clarified and homogeneous with good fluidity and the results are shown in **Fig. 5A**. The MM droplets under the transmission electron microscope were round with clear edges and the particle size met the requirements, and the results were shown in **Fig. 5B**.

3.3.2 Types of microemulsion

After adding Sudan III and methylene blue to MM, methylene blue diffused faster, so MM was judged to be O/W type, and the results are shown in **Fig. 5C**.

3.3.3 Particle size and zeta potential of microemulsion

The mean value of particle size of MM was 16.6100 ± 0.0265 nm, the mean value of PDI was 0.0883 ± 0.0045, and the zeta potential of MM was -2.3300 ± 0.3020 mV. The results are shown in **Figs. 5D** and **5E**.

Microemulsions typically have a particle size of 10 – 100 nm. Their small size induces vigorous Brownian motion, preventing gravitational settling. Additionally, the larger specific surface area from small particles promotes tight interfacial adsorption of emulsifiers, strengthening the interfacial film and reducing droplet coalescence risk[26]. Specifically, a PDI < 0.1 indicates a monodisperse system with uniform particle size distribution, whereas a PDI > 0.3 signifies a polydisperse system with highly heterogeneous particle size distribution[27]. Zeta potential refers to the potential difference between the charged surface of microemulsion particles and the surrounding medium. In the optimal microemulsion formulation, EL-40, a non-ionic polymeric emulsifier, features long polyoxyethylene segments that extend into the aqueous phase. Upon adsorption onto the surface of emulsion droplets, these segments create a steric hindrance effect, which both reduces particle mobility and impedes droplet aggregation [28]. Consequently, the microemulsion retains good stability during storage even when the system exhibits a low Zeta potential[29, 30].

3.3.4 Stability study of microemulsion

3.3.4.1 Physical stability of microemulsion

After subjecting the MM to high-speed centrifugation, no stratification was observed and its appearance remained clear, which was indicative of its excellent centrifugal stability.

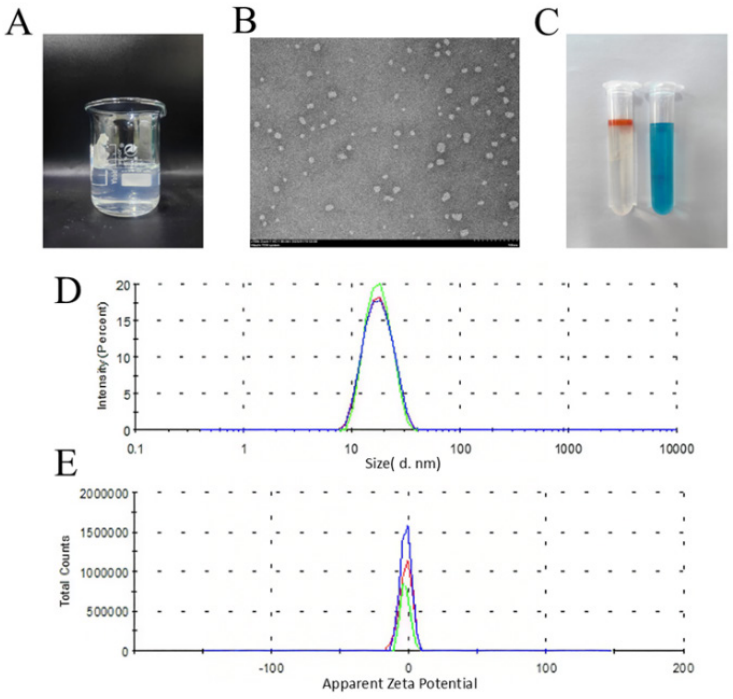


Fig. 5 Characterization of myrrh essential oil microemulsions. A: Image of microemulsions, B: Transmission Electron Microscopy image, C: Microemulsion type identification diagram, D: Microemulsion particle size (n = 3), E: Microemulsion particle Zeta potential distribution image (n = 3).

3.3.4.2 Thermodynamic stability of microemulsion

After the heating-cooling and freezing-thawing cycle experiments on MM, its microemulsion appearance persisted in being clear and without any sign of delamination. The results are shown in **Fig. 6**, indicating that MM has good thermodynamic stability.

3.3.4.3 Accelerated stability of microemulsion

To test the conductivity, particle size and to observe the appearance. The results are shown in **Table 2**.

3.3.5 Determination of essential oil retention in MEO and MM in thermal environments

Figure 7 shows the essential oil retention rates in MEO and MM. Under the condition of 60 °C, the essential oil retention rate of the MM group was significantly higher than that of the MEO group at different storage times (1 h, 3 h, and 8 h). Specifically, at 8 h, the retention rate of the MEO group was only 34.67%, while that of the MM group reached 58.67%. This indicates that MEO formulated into microemulsions can significantly reduce volatilization and improve stability.

3.4 Evaluation of the efficacy of myrrh essential oil microemulsion formulations

3.4.1 Behavioral observations

The Differences in DAI scores, body weight changes and colon lengths of mice in each group are illustrated in **Fig. 8**. The mice in the Control group exhibited a steady weight gain over time. In contrast, mice in the model group, MEO group, and MM group developed diarrhea starting from the days 2-3 of the modeling. Some of these mice even presented with thinning of the feces and a consequent decline in body weight. Blood was observable in their feces on day 4. Nevertheless, on day 5, the fecal conditions of mice in MEO and MM group mice had returned to normal. In terms of colon length, the colon of mice in the Control group was the longest, the Model mice had shorter colon length, while the MEO and MM mice had longer colon length. This indicates that both MEO and MM can effectively alleviate ulcerative colitis in mice.

Table 2 Microemulsion accelerated stability results ($\bar{X} \pm SD$, n = 3).

Time/Month	Particle Size (nm)	Conductivity (μs·cm^{-1})	Appearances
0	16.61 ± 0.03	214.38 ± 1.25	homogeneous and transparent
1	17.05 ± 0.16	212.53 ± 0.91	homogeneous and transparent
2	17.81 ± 0.07	210.17 ± 1.64	homogeneous and transparent
3	18.26 ± 0.19	199.98 ± 2.33	homogeneous and transparent

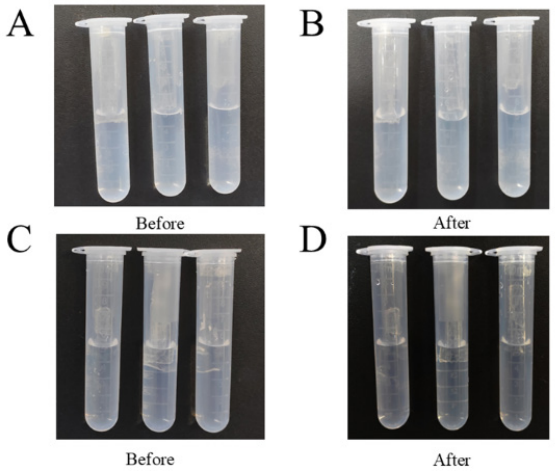


Fig. 6 Experimental diagram of heating-cooling and freezing-thawing cycles of myrrh essential oil microemulsions (n = 3). A: Before heating-cooling cycle experiment, B: After heating-cooling cycle experiment, C: Before freezing-thawing cycle experiment, D: After freezing-thawing cycle experiment.

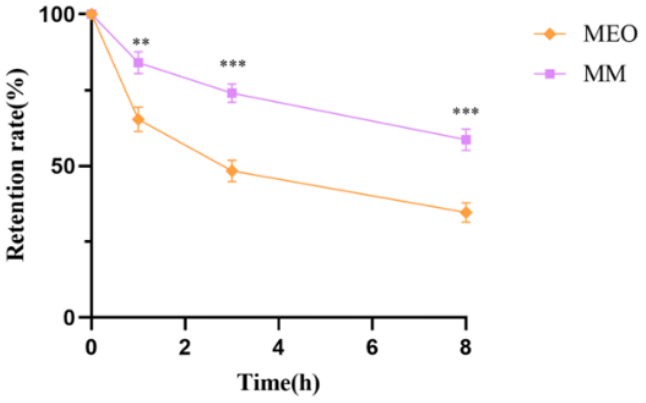


Fig. 7 Determination of essential oil retention in MEO and MM in thermal environments ($\bar{X} \pm SD$, n = 3). Notes: $^{**}p < 0.01$, $^{***}p < 0.001$ compared with the MEO group.

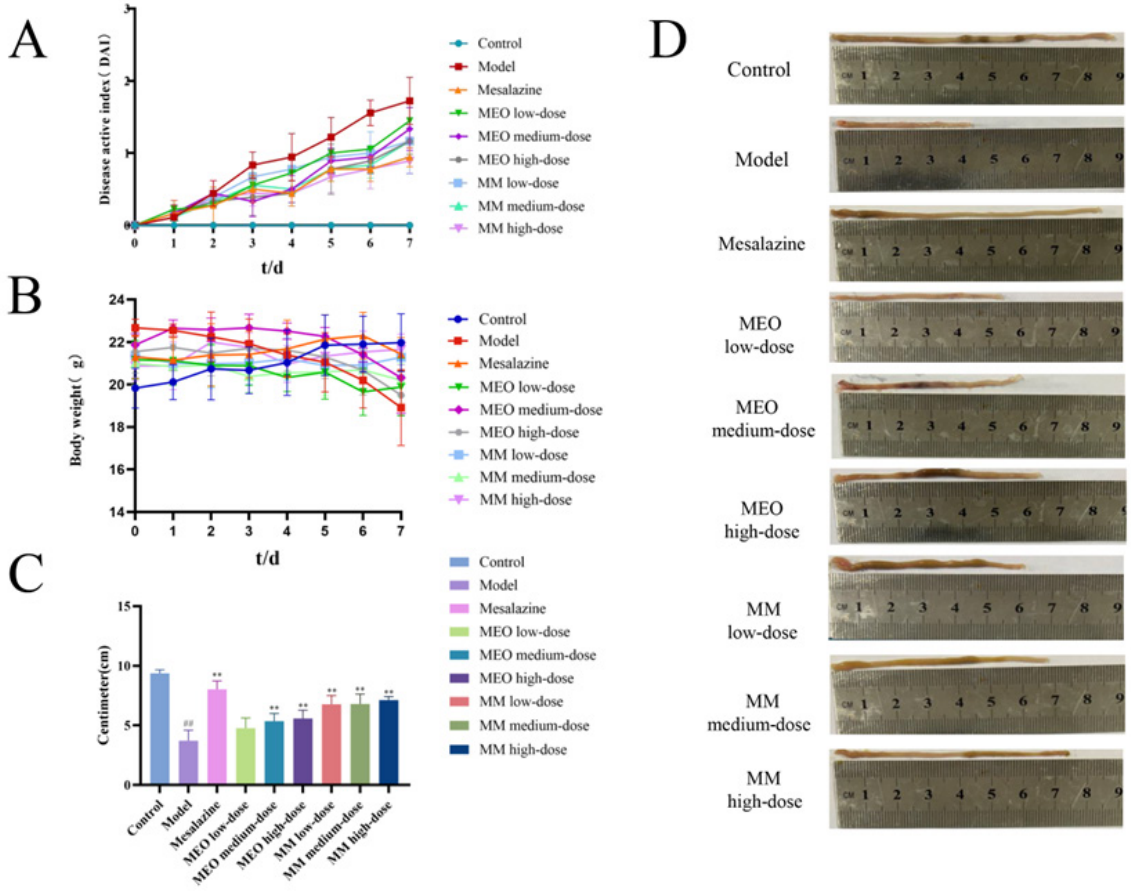


Fig. 8 DAI score and colon morphology in UC mice ($\overline{X}$ ± SD, n = 6). A: DAI scores for each group of mice, B: Changes in body weight of mice in each group, C: Colon length in each group of mice, D: Colonic morphology of mice in each group. Notes: ##$p < 0.01$ compared to the control group. **$p < 0.01$ compared to the model group

3.4.2 HE Staining

The HE staining results of colonic tissues of mice in each group are shown in **Fig. 9A**. In the Control group, the structure of colonic tissues of mice was normal. Conversely, in the Model group, the overall structure of colonic tissues of mice was obviously abnormal, with a large number of inflammatory cells infiltrating the tissues. In the medium-dose and high-dose of the MEO group, the tissue structure was basically normal, with only a small number of inflammatory cells infiltrating. The area of necrosis in the medium-dose of the MEO group was almost very small, and there was no necrosis in the high-dose of the MEO group. Within the MM group, both the middle and high doses led to a normalization of the tissue structure, with tiny inflammatory cell infiltration and no necrosis. This indicates that MEO and MM can improve the condition of ulcerative colitis, and the MM high-dose group is more effective in inhibiting ulcerative colitis.

3.4.3 ELISA

The levels of TNF-α and IL-1β within the serum of mice were detected using ELISA kits (the higher the levels of these two factors, the more severe the inflammation). The results are shown in **Figs. 9B** and **9C**, where the levels of TNF-α and IL-1β were significantly higher in the Model group compared to the Control group. Compared with the Model group, the levels of TNF-α and IL-1β in the Mesalazine, MEO and MM groups were decreased to different degrees, and the comparison between the MEO and MM groups showed that the MM group had a better effect in inhibiting the release of TNF-α and IL-1β factors. In conclusion, MEO and MM can effectively reduce the expression of inflammatory factors in UC mice, and the high dose group of MM achieves the greatest effect.

3.4.4 IHC

The immunohistochemical results are shown in **Fig. 10**. A large number of positively stained cells were observed in

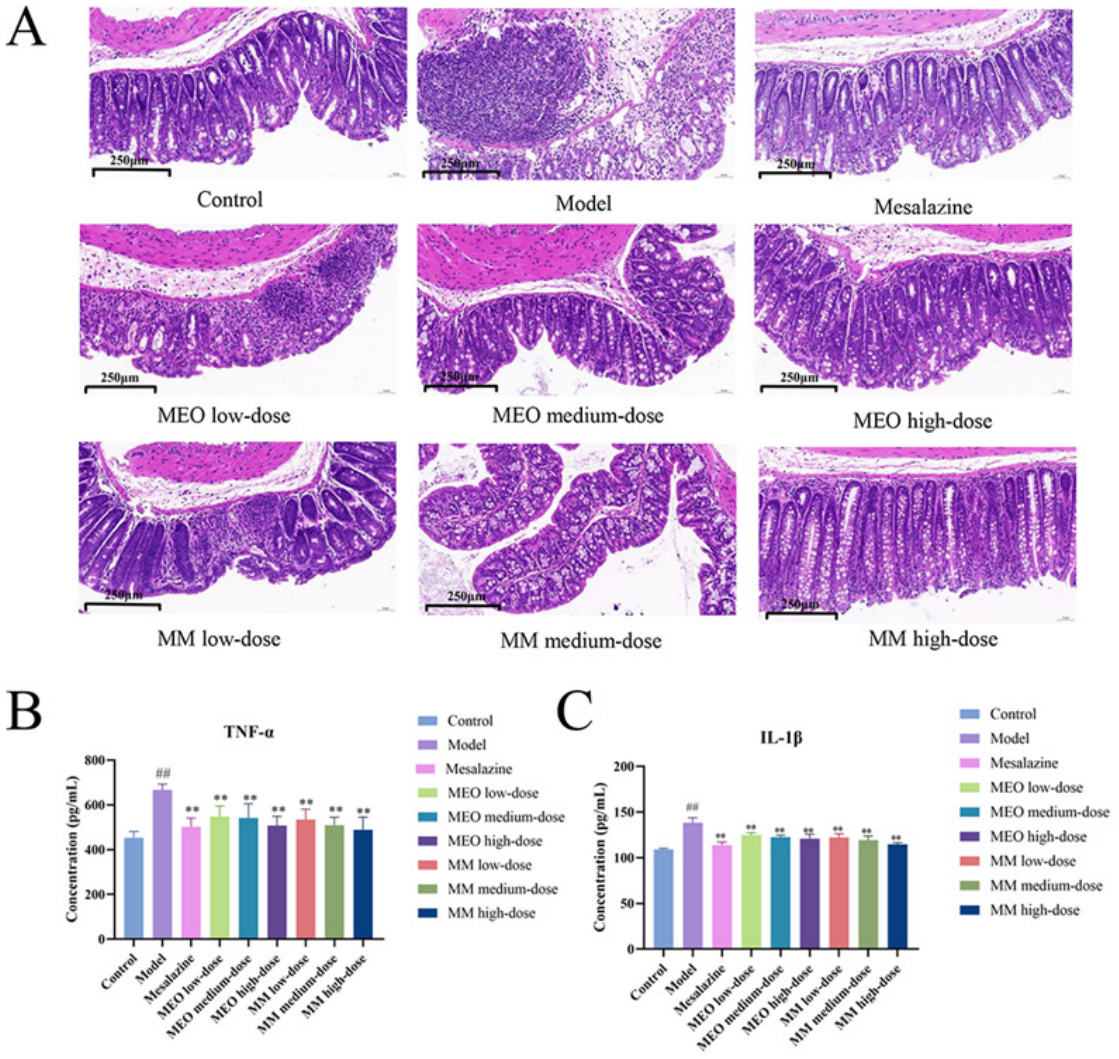


Fig. 9 HE staining and the expression of TNF-α and IL-1ß. A: HE staining of the colon of mice (200×), B: Expression of TNF-α, C: Expression of IL-1ß ($\bar{X}$ ± SD, n = 6). Notes: ##p < 0.01 compared to the control group. **p < 0.01 compared to the model group.

the colon tissue of mice in the Model group. The area of positive cell staining in the colon tissue of the MEO group and the MM group was reduced to varying degrees. Comparison of the MEO and MM groups showed that the MM reduced the expression levels of p-JNK and p-ERK to a greater extent.

4 Discussion

GC-MS analysis identified the primary constituents of myrrh essential oil as Furanoeudesma-1,3-diene, Curzerene, Lindestrene, Isolongifolene and ß-Elemen. Among these, Furanoeudesma-1,3-diene acts as a specific agonist of the opioid δ receptor, exerting potent analgesic effects[31]; it also exhibits high affinity for COX-2, conferring anti-inflammatory activity[32]. Figueiredo et al. demonstrated that Curzerene induces apoptosis in human colon cancer cells, thereby contributing to the treatment of colonic disorders[33], while Zhao et al. confirmed its antioxidant properties via TLC separation coupled with in-situ DPPH bioautographic assay[34]. Additionally, Li et al. revealed that Isolongifolene exerts anti-inflammatory and antioxidant effects through regulation of the AMPK-PGC1α signaling pathway[35, 36]. Lindestrene also possesses anti-inflammatory and analgesic activities due to its strong binding affinity for COX-1 [37]. Whereas ß-Elemen exerts anti-inflammatory and immunomodulatory effects by inhibiting excessive macrophage activation and reducing

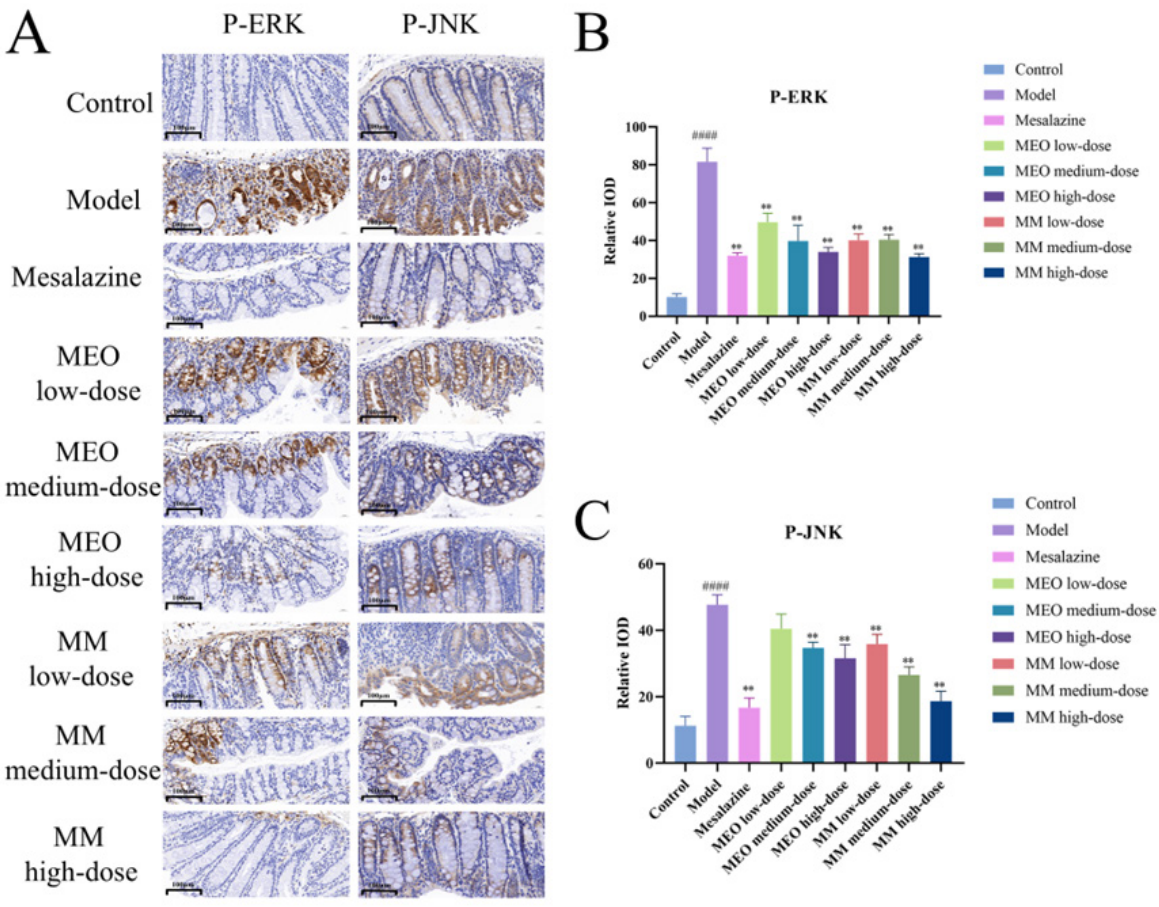


Fig. 10 Expression of p-JNK and p-ERK in UC mice ($\bar{X} \pm SD$, n = 3). A: Effect of MEO and MM on p-ERK and p-JNK protein levels in DSS-induced colon tissue, B: p-ERK protein levels in colonic tissues of mice in each group, C: p-JNK protein levels in the colonic tissues of mice in each group. Notes: $^{\#\#\#\#}p < 0.0001$ compared to the control group. $^{**}p < 0.01$, $^{***}p < 0.001$, $^{****}p < 0.0001$ compared to the model group.

the release of inflammatory mediators[38, 39]. The synergistic action of these components is likely the material basis underlying the anti-ulcerative colitis (UC) efficacy of myrrh essential oil.

Essential oils exhibit low bioavailability in their free form due to their high volatility and strong lipophilicity. Microemulsions, however, offer advantages: their nano-scale particle size enhances water solubility and reduces volatile loss, while the surfactant-based interfacial film encapsulates essential oil components, protecting them from gastrointestinal degradation[40-42]. Consequently, this study formulated myrrh essential oil into microemulsions, with formulation screening and stability tests ensuring consistent physicochemical properties during storage and application.

In a DSS-induced UC mouse model, both myrrh essential oil and its microemulsions alleviated weight loss, diarrhea, and bloody stool. HE staining revealed reduced colonic mucosal damage and inflammatory cell infiltration following treatment, indicating mitigation of intestinal pathological injury. IHC analysis demonstrated decreased p-JNK and p-ERK levels in treated groups, suggesting intestinal barrier repair. ELISA further confirmed reduced pro-inflammatory cytokine levels (TNF-α, IL-1β), implying therapeutic effects via regulation of immune-inflammatory responses. Moreover, at equivalent doses, the microemulsion group exhibited significantly superior efficacy compared to the free essential oil group. This discrepancy may be attributed to the fact that preparing MEO into microemulsion reduces the volatilization of essential oil and improves its stability[43, 44]. Furthermore, the small particle size of microemulsions enables them to enhance intestinal absorption, thereby boosting bioavailability[28, 45]. However, this study did not investigate the in vivo pharmacokinetic profile of the microemulsions, precluding direct confirmation of improved bioavailability—a topic warranting further research.

5 Conclusion

This study confirmed that myrrh essential oil and its microemulsion can treat ulcerative colitis in mice. As a new drug delivery system, the microemulsion can significantly enhance the efficacy of the essential oil by improving its physicochemical properties. These experiments will be helpful for the discovery of new therapeutic targets, methods and drugs for the treatment of UC.

CRediT Authorship Contribution Statement

Mengmeng Wang: Writing – review & editing, Writing – original draft, Validation, Investigation, Formal analysis, Conceptualization. Tiantian Tang: Writing – review & editing, Validation. Mei Liu: Software. Zihao Niu: Software. Le Zhang: Software. Xuan Wang: Software, Methodology, Data curation. Ning Xia: Software, Methodology. Jie Wang: Software, Methodology. Jinhui Wang: Software, Methodology, Data curation. Chao Chen: Software, Data curation. Xiaoxiao Ge: Software. Qin Chen: Software. Shihao Zhang: Software. Yundong Xie: Methodology. Huanxian Shi: Software. Chongbo Zhao: Software. Junbo Zou: Validation. Dongyan Guo: Validation, Investigation. Yajun Shi: Software, Methodology. Ming Yang: Software, Methodology. Xiaofei Zhang: Writing – review & editing, Supervision, Funding acquisition, Conceptualization. Jing Sun: Investigation, Funding acquisition, Formal analysis.

Funding

This project has been supported by the National Key Research and Development Program of China (2021YFD1601004,2023YFD1600402,2023YFD1600403); Shaanxi Provincial Key Research and Development Program Project (2024CY-JJQ-36); Xi'an Science and Technology Plan Project(20231H-JSJ0-0007); Inner Mongolia Autonomous Region Science and Technology Program (2022YFSH0001); Shaanxi Provincial Traditional Chinese Medicine Science and Technology Innovation Team (TZKN-CXTD-03); Shaanxi Provincial Department of Science and Technology Project (2024ZC-YYDP-110, 2025JC-YBMS-1056); Shaanxi Province Xianyang City Science and Technology Bureau Project (L2024-QCY-ZYYJJQ-X28); Shaanxi Provincial Administration of Traditional Chinese Medicine (ZYJXG-Y23005); Key Technological Innovation Team for Industrialization of Aromatic Traditional Chinese Medicine; Shaanxi Provincial Engineering Research Center for Traditional Chinese Medicine Aromatic Industry; Key Discipline of High Level Traditional Chinese Medicine in Shaanxi Province， Traditional Chinese Medicine Processing; Department of Education of Shaanxi Province Key Research Project (No. 24JR054).

Declaration of Competing Interest

Authors declare no conflict of interest.

Data Availability

Data will be made available on request.

Supporting Information

This material is available free of charge via the Internet at doi: 10.5650/jos.ess25047.

References

1) Saez, A.; Herrero-Fernandez, B.; Gomez-Bris, R.; Sánchez-Martinez, H.; Gonzalez-Granado, J.M. Pathophysiology of inflammatory bowel disease: Innate immune system. *Int. J. Mol. Sci.* **24**, 1526 (2023).
2) Nakase, H.; Sato, N.; Mizuno, N.; Ikawa, Y. The influence of cytokines on the complex pathology of ulcerative colitis. *Autoimmun. Rev.* **21**, 103017 (2022).
3) Mitsialis, V.; Wall, S.; Liu, P.; Ordovas-Montanes, J.; Parmet, T. et al. Single-cell analyses of colon and blood reveal distinct immune cell signatures of ulcerative colitis and Crohn's disease. *Gastroenterology* **159**, 591-608.e10 (2020).
4) Xu, L.; He, B,; Sun, Y.; Li, J.; Shen, P. et al. Incidence of inflammatory Bowel disease in urban China: A nationwide population-based study. *Clin. Gastroenterol. Hepatol.* **21**, 3379-3386.e3329 (2023).
5) Zang, L.; Li, Y.; Hao, H.; Liu, J.; Cheng, Y. et al. Efficacy and safety of umbilical cord-derived mesenchymal stem

cells in Chinese adults with type 2 diabetes: A single-center, double-blinded, randomized, placebo-controlled phase II trial. *Stem Cell Res. Ther.* **13**, 180 (2022).
6) Zheng, S.; Xue, T.; Wang, B.; Guo, H.; Liu, Q. Chinese medicine in the treatment of ulcerative colitis: The mechanisms of signaling pathway regulations. *Am. J. Chin. Med.* **50**, 1781-1798 (2022).
7) Kuck, K.; Unterholzner, A.; Lipowicz, B.; Schwindl, S.; Jürgenliemk, G. et al. Terpenoids from myrrh and their cytotoxic activity against HeLa cells. *Molecules* **28**, 1637 (2023).
8) Kieliszek, M.; Edris, A.; Kot, A.M.; Piwowarek, K. Biological activity of some aromatic plants and their metabolites, with an emphasis on health-promoting properties. *Molecules* **25**, 2478 (2020).
9) Holleran, G.; Scaldaferri, F.; Gasbarrini, A.; Currò, D. Herbal medicinal products for inflammatory bowel disease: A focus on those assessed in double-blind randomised controlled trials. *Phytother. Res.* **34**, 77-93 (2020).
10) Batiha, G.E.; Wasef, L.; Teibo, J.O.; Shaheen, H.M.; Zakariya, A.M. et al. Commiphora myrrh: A phytochemical and pharmacological update. *Naunyn Schmiedebergs Arch. Pharmacol.* **396**, 405-420 (2023).
11) Zhao, Y.; Wang, Y.; Zhang, Z.; Li, H. Advances in controllable release essential oil microcapsules and their promising applications. *Molecules* **28**, 4979 (2023).
12) Pang, M.; Cao, L.; Kang, S.; Jiang, S.; Cao, L. Controlled release of flavor substances from sesame-oil-based oleogels prepared using biological waxes or monoglycerides. *Foods* **10**, 1828 (2021).
13) Hogenbom, J.; Istanbouli, M.; Faraone, N. Novel ß-cyclodextrin and catnip essential oil inclusion complex and its tick repellent properties. *Molecules* **26**, 7391 (2021).
14) Ellboudy, N.M.; Elwakil, B.H.; Shaaban, M.M.; Olama, Z.A. Cinnamon oil-loaded nanoliposomes with potent antibacterial and antibiofilm activities. *Molecules* **28**, 4492 (2023).
15) Rehman, R.; Hussain, M.; Muzaffar, R.; Bano, A.; Ahmed, M. et al., Eucalyptus essential oil based nanoemulsions: Preparation and biological activities. *Chem. Biodivers.* **21**, e202400406 (2024).
16) Yong, Z.; Xingqi, W.: Jie, H.; Rongfeng, H.; Xiaoqin, C. Formulation, production, in vitro release and in vivo pharmacokinetics of cinnamaldehyde sub-micron emulsions. *Pharm. Dev. Technol.* **25**, 676-685 (2020).
17) Luna-Canales, I.C.; Delgado-Buenrostro, N.L.; Chirino, Y.I.; Nava-Arzaluz, G.; Piñón-Segundo, E. et al. Curcumin-loaded microemulsion: Formulation, characterization, and in vitro skin penetration. *Drug Dev. Ind. Pharm.* **49**, 42-51 (2023).
18) Thakur, D.; Kaur, G.; Puri, A.; Nanda, R. Therapeutic potential of essential oil-based microemulsions: Reviewing State-of-the-art. *Curr. Drug Deliv.* **18**, 1218-1233 (2021).
19) Li, M.; Zhang, H.; Wu, Z.; Zhu, Z.; Jia, X. DPD Simulation on the transformation and stability of O/W and W/O microemulsions. *Molecules* **27**, 1361 (2022).
20) Scomoroscenco, C.; Teodorescu, M.; Burlacu, S.G.; Gîfu, I.C.; Mihaescu, C.I. et al. Synergistic antioxidant activity and enhanced stability of curcumin encapsulated in vegetal oil-based microemulsion and gel microemulsions. *Antioxidants (Basel)* **11**, 854 (2022).
21) Hou, X.; Sang, Y.; Dong, L. The improved effect and its mechanism of phytic acid on DSS-induced UC mice. *Life Sci.* **311**(Pt A), 121139 (2022).
22) Lin, Y.; Su, J.; Wang, M.; Li, Y.; Zhao, Z. et al. Hypericumsampsonii attenuates inflammation in mice with ulcerative colitis via regulation of PDE4/PKA/CREB signaling pathway. *J. Ethnopharmacol.* **296**, 115447 (2022).
23) Zheng, Y.; Liang, C.; Li, Z.; Chen, J.; Chen, Z. et al. Study on the mechanism of Huangqin Decoction on rats with ulcerative colitis of damp-heat type base on mtDNA, TLR4, p-PI3K, p-Akt protein expression and microbiota. *J Ethnopharmacol.* **295**: p. 115356 (2022).
24) Ahamad, S.R.; Al-Ghadeer, A.R.; Ali, R.; Qamar, W.; Aljarboa, S. Analysis of inorganic and organic constituents of myrrh resin by GC-MS and ICP-MS: An emphasis on medicinal assets. *Saudi Pharm. J.* **25**, 788-794 (2017).
25) de Jesus, E.N.S.; Tavares, M.S.; Barros, P.A.C.; Miller, D.C.; da Silva, P.I.C. et al. Chemical composition, antinociceptive and anti-inflammatory activities of the curzerene type essential oil of Eugenia uniflora from Brazil. *J. Ethnopharmacol.* **317**, 116859 (2023).
26) Demirci Kayiran, S.; Guven Bolgen, U.M.; Cevikelli, T.; Kızılyıldırım, S.; Yıldır, B. et al. Chemical composition and antibacterial properties of microemulsion and microemulgel formulations containing *Lavandula angustifolia* Mill. essential oils. *Ind. Crops Prod.* **226**, 120654 (2025).
27) Shah, J.; Nair, A.B.; Jacob, S.; Patel, R.K.; Shah, H. et al. Nanoemulsion based vehicle for effective ocular delivery of moxifloxacin using experimental design and pharmacokinetic study in rabbits. *Pharmaceutics* **11**, 230 (2019).
28) Huang, Y.; Wang, P.; Zhao, P.; Cheng, W.; Fu, H. et al. ROS/Thermo dual-sensitive hydrogel loaded with a nanoemulsion of patchouli essential oil for ulcerative colitis. *Int. J. Biol. Macromol.* **281**, 136542 (2024).
29) Jalali Jivan, M.; Abbasi, S. Nano based lutein extraction from marigold petals: Optimization using different

surfactants and co-surfactants. *Heliyon* **5**, e01572 (2019).
30) Huang, Y.; Ni, N.; Zhao, L.; Zhang, J.; Shen, L. The preparation, evaluation and phase behavior of linker-based coix seed oil microemulsion. *J. Mol. Liq.* **319**, 114314 (2020).
31) Dolara, P.; Luceri, C.: Lodovici, M.; Ghelardini, C.; Aiolli, S. et al. Furanoeudesma-1,3-diene, A sesqiterpene from MYRRH, is a specific agonist of opiod delta receptors. *Pharmacol. Res.* **31**, 34 (1995).
32) Al-Radadi, N.S. Single-step green synthesis of gold conjugated polyphenol nanoparticle using extracts of Saudi's myrrh: Their characterization, molecular docking and essential biological applications. *Saudi Pharm. J.* **30**, 1215-1242 (2022).
33) Figueiredo, P.L.B.; Pinto, L.C.; da Costa, J.S.; da Silva, A.R.C.; Mourão, R.H.V. et al. Composition, antioxidant capacity and cytotoxic activity of Eugenia uniflora L. chemotype-oils from the Amazon. *J. Ethnopharmacol.* **232**, 30-38 (2019).
34) Zhao, J.; Zhang, J.S.; Yang, B.; Lv, G.P.; Li, S.P. Free radical scavenging activity and characterization of sesquiterpenoids in four species of Curcuma using a TLC bioautography assay and GC-MS analysis. *Molecules* **15**, 7547-7557 (2010).
35) Balakrishnan, R.; Vijayraja, D.; Mohankumar, T.; Manimaran, D.; Ganesan, P. et al. Isolongifolene mitigates rotenone-induced dopamine depletion and motor deficits through anti-oxidative and anti-apoptotic effects in a rat model of Parkinson's disease. *J. Chem. Neuroanat.* **112**, 101890 (2021).
36) Li, J.; Li, J.; Fang, H.; Yang, H.; Wu, T. et al. Isolongifolene alleviates liver ischemia/reperfusion injury by regulating AMPK-PGC1α signaling pathway-mediated inflammation, apoptosis, and oxidative stress. *Int. Immunopharmacol.* **113**(Pt A), 109185 (2022).
37) Al-Radadi, N.S. Single-step green synthesis of gold conjugated polyphenol nanoparticle using extracts of Saudi's myrrh: Their characterization, molecular docking and essential biological applications. *Saudi Pharm. J.* **30**, 1215-1242 (2022).
38) Gong, Q.; Wang, Y.; Liu, F.; Huang, Y.; Li, L. et al. ß-elemene attenuates IRI-AKI by inhibiting inflammation and apoptosis via suppression of the TLR4/MyD88/NF-κB/MAPK signal axis activation. *Mol. Med. Rep.* **32**, 221 (2025).
39) Zhang, S.; Xing, Z.; Ke, J. Using ß-Elemene to reduce stemness and drug resistance in osteosarcoma: A focus on the AKT/FOXO1 signaling pathway and immune modulation. *J. Bone Oncol.* **50**, 100655 (2025).
40) Saesue, K; Matwangsang, S.; Rungsang, T.; Khorana, N.; Thong-on, P. et al. Deep eutectic-based microemulsion: A multifunctional system for enhancing extraction efficiency, stability and antityrosinase, antioxidant activities of oxyresveratrol from Artocarpus lakoocha Roxb. *J. Mol. Liq.* **436**, 128253 (2025).
41) Kongpol, K.; Sermkaew, N.; Makkliang, F.; Khongphan, S.; Chuaboon, L. et al. Extraction of curcuminoids and ar-turmerone from turmeric (*Curcuma longa* L.) using hydrophobic deep eutectic solvents (HDESs) and application as HDES-based microemulsions. *Food Chem.* **396**, 133728 (2022).
42) Callender, S.P.; Mathews, J.A.; Kobernyk, K.; Wettig, S.D. Microemulsion utility in pharmaceuticals: Implications for multi-drug delivery. *Int. J. Pharm.* **526**, 425-442 (2017).
43) Nery Dos Santos, Q.; Teles, D.C.S.; de Araujo, G.R.S.; Lima, O.V.A.; Silva, L.A.S. et al. Microemulsions strongly promoted the activity of α-bisabolol against different Leishmania species and its skin permeation. *Exp. Parasitol.* **265**, 108808 (2024).
44) Wang, J.; Jia, Y.; Xia, N.; Wang, X,; Zhou, P. et al. Rosemary essential oil microemulsion prevents DSS-induced intestinal injury in mice by modulating IL-17 signaling pathway. *J. Funct. Foods* **116**, 106180 (2024).
45) Tamizmaran, V.; Mannur, V.S.; Koli, R.; Biradar, P. Novel intranasal fisetin-loaded mucoadhesive microemulsion for Schizophrenia management: A nanotherapeutic approach to enhance brain bioavailability and improved efficacy. *Mol. Pharm.* **22**, 4293-4313 (2025).

CC BY 4.0 (Attribution 4.0 International). This license allows users to share and adapt an article, even commercially, as long as appropriate credit is given. That is, this license lets others copy, distribute, remix, and build upon the Article, even commercially, provided the original source and Authors are credited.